A&A 425, 171–177 (2004)
DOI: 10.1051/0004-6361:20035922

Astronomy & Astrophysics

HD 153720 – A SB2 system with twin metallic-line components⋆,⋆⋆

A. V. Yushchenko[1,2], V. F. Gopka[2], V. L. Khokhlova[3], D. L. Lambert[4], C. Kim[5], and Y. W. Kang[1]

[1] Department of Astronomy, Sejong University, Seoul, 143-747, Korea
e-mail: yua@arcsec.sejong.ac.kr; kangyw@sejong.ac.kr
[2] Odessa Astronomical Observatory, Odessa National University, Park Shevchenko, Odessa, 65014, Ukraine
e-mail: yua@odessa.net; gopkavera@mail.ru
[3] Deceased (Institute of Astronomy, Russian Academy of Sciences, Pyatnitskaya ul. 48, Moscow, 109017, Russia)
[4] The W. J. McDonald Observatory, University of Texas, Austin, TX 78712, USA
e-mail: dll@astro.as.utexas.edu
[5] Department of Earth Science Education, Chonbuk National University, Chonju 561-756, Korea
e-mail: chkim@astro.chonbuk.ac.kr

Received 20 December 2003/ Accepted 25 May 2004

Abstract. We report the results of abundance determinations for the components of the SB2 star HD 153720 from high resolution (R = 60 000) echelle high signal-to-noise spectra of the wavelength region 3595−10 260 Å taken with the 2.7 m telescope of the McDonald Observatory We found the values of the atmospheric parameters of the primary to be effective temperature $T_{\rm eff}$ = 7425 K and surface gravity log g = 4.0 cgs, and of the secondary to be $T_{\rm eff}$ = 7125 K and log g = 3.9 cgs. The microturbulent velocity is $v_{\rm micro}$ = 2.7 km s^{-1} for both components, and the projected rotational velocity is $v \sin i$ = 15 km s^{-1} also for both components. The abundances of about 20 elements were determined with the method of spectrum synthesis. The components of HD 153720 are metallic-line stars. Possible inconsistencies between old and new measurements of radial velocities may be explained by the existence of third body in this system. A review of recent high resolution spectral observations of eight A4-F1 binaries shows that only one of these systems can be classified as normal.

Key words. stars: abundances – stars: atmospheres – stars: evolution – stars: chemically peculiar – stars: binaries: spectroscopic – stars: individual: HD 153720

1. Introduction

HD 153720 (BD+75 608) of magnitude $V = 6\overset{\rm m}{.}82$ and spectral class F0 was first noted by Young (1942) to be a spectroscopic binary. The orbit of this unevolved double-lined spectroscopic binary was determined by Heard & Hurkens (1975) using forty-six 12 Å/mm spectrograms (1971−1974). They did not mention the chemical composition of the components, but pointed out that there was no difficulty in distinguishing primary from secondary, and that the difference in their line strengths was not great. Budaj (1996) used HD 153720 as an example of a binary with normal components, i.e., neither star exhibited chemical peculiarities. We observed HD 153720 as part of an investigation of atmospheric abundances of SB2 systems whose components have equal masses and are unevolved main-sequence stars.

It was started by one of the authors of this paper (Vera L. Khokhlova). She died last September (2003); this and the next papers of the series are devoted to her memory.

The stars of this program studied to date are AR Aur (Khokhlova et al. 1995), 46 Dra (Tsymbal et al. 1998) and 66 Eri (Yushchenko et al. 1999). Preliminary results for HD 153720 were reported by Yushchenko et al. (2002).

One might suppose that unevolved stars of equal mass comprising a binary should have very similar, if not identical, compositions. This supposition is questionable, however, for main sequence A and F stars for which chemical peculiarities are extremely common. Do the components of HD 153720 have the same chemical composition?

Our previous investigations of the chemical composition of the individual components of A-type binaries showed strong differences for some elements. For AR Aur (Khokhlova et al. 1995), a system with mass ratio M_A/M_B = 1.09, the abundances of the majority of the elements are similar, but on the whole differ from the normal (i.e., solar) values. For Al, Ni, Pt, and Hg, there are differences between the components of more than 1 dex. A similar situation was found for 46 Dra (Tsymbal et al. 1998) with mass ratio M_A/M_B = 1.14: the abundances are similar for all elements except Al, Ga, Sr, Pt. A more interesting case is 66 Eri (Yushchenko et al. 1999), with M_A/M_B = 0.98 (Yushchenko et al. 2001). In the spectrum of the main

⋆ Based on observations obtained at the 2.7-m telescope of the McDonald Observatory.
⋆⋆ The data are only available in electronic form at http://www.edpsciences.org

component, only lines of elements with $Z \leq 26$ and barium lines were found. The spectrum of the secondary component showed numerous lines of heavy elements, indicating overabundances of these elements of between 2 and 6 dex. A similar binary system was analysed by Catanzaro et al. (2003): HD 191110 ($M_A/M_B = 1.08$). We may mention also the paper by Adelman et al. (1998) on 46 Dra, where abundance differences for Sr and Pt of more than 1 dex exist between the primary and the secondary.

HD 153720 was originally chosen as a comparison star for our program. We expected HD 153720 to be a system of unevolved components with solar chemical composition. Our abundance analyses, the first for the star, show that HD 153720 is a system of metallic-line stars.

2. Spectral observations and data reduction

The two spectra of HD 153720 used in this study were obtained in 1996 with the echelle spectrograph of the 2.7-m McDonald Observatory telescope (Tull et al. 1995). Sixty-three spectral orders covered the wavelength range 3895−10 260 Å at a resolving power of 60 000 and signal to noise ratio > 200. The spectral coverage is incomplete beyond about 5600 Å.

Initial reduction of the spectra was done at the University of Texas by V. Woolf with the participation of V. L. Khokhlova using the KPNO-IRAF software package. Further reduction and calculations were performed using the URAN (Yushchenko 1998) package. The location of the continuum was determined taking into account the synthetic spectrum. The heliocentric Julian dates of our spectra can be found in Table 4. It should be noted that one of the spectra was obtained at a time when the spectral lines of the components were unresolved at a separation of less than 5 km s^{-1}.

This spectrum was used only to provide an estimate of radial velocity with an error near 1 km s^{-1}. The spectrum with the lines separated by 104 km s^{-1} was used for the determination of atmospheric parameters and for abundance calculations.

3. Radial velocities and orbital elements

To measure the radial velocities of the components of HD 153720 we selected unblended lines of neutral iron. The data are only available in electronic form at `http://www.edpsciences.org`. The results are listed in Table 4. This table gives the heliocentric Julian dates of the observations, the corresponding orbital phases (according to the ephemerides from Table 5), designations for the binary components, the mean radial velocity, the number of measured spectral lines, and the errors of the mean.

Our data and 46 observations of Heard & Hurkens (1975) permit us to determine new orbital elements of the system. In Table 5 we show two sets of new orbital elements and the Heard & Hurkens (1975) result. The residuals of our radial velocity values from the first solution are near 4 km s^{-1} and significantly larger than the errors of our measurements but may approximate the errors of of the Heard & Hurkens (1975) measurements. The residuals are decreased if we correct our radial velocities by −4 km s^{-1}. The second solution was made with our velocities shifted by 4 km s^{-1} with respect to the earlier results.

Table 1. Radial velocities of components of HD 153720 .

JD_{hel}	Phase	Component	V_r km s^{-1}	N	σ km s^{-1}
2 450 206.9208	0.413	*A*	−10:		1
.9208	0.413	*B*	−10:		1
2 450 209.9518	0.689	*A*	−60.9	60	0.1
.9518	0.689	*B*	+43.1	46	0.1

3.1. Third body?

The 4 km s^{-1} difference may be explained in two ways. First, it is quite common to attribute such a difference to a third body in the system. In this case, the amplitude of the variations of the γ-velocity is at least 3 km s^{-1}. The orbital period of a third body should be significantly larger than 3 years – the time interval covered by the observations of Heard & Hurkens (1975). If the period is of the order of several dozen years, the mass of the third body can be less than a solar mass. Second, a systematic error in the old observations of Heard & Hurkens (1975) may exist. However, for 66 Eri we found no systematic shift between our observations (Yushchenko et al. 2001) and those of Young (1976). The observations of Heard & Hurkens (1975) were made with the 1.88 m telescope of the David Dunlap Observatory. There is no evidence for a systematic shift between the radial velocities obtained at the David Dunlap and modern measurements with coudeé spectrographs at the McDonald Observatory: see, for example Scarfe et al. (1994), and Fekel & Tomkin (1993).

We found no evidence of third light in our analysis of chemical abundances in the visual spectral region. Indeed, the predicted combined flux of the two stars is consistent with the measured fluxes from the ultraviolet (TD1 observations, Thompson et al. 1978), through the optical (*UBV* photometry), to the infrared (IRAS observations, Moshir et al. 1989). We conclude that, if a third body exists, it must be a low mass main sequence star.

4. Atmospheric parameters of the components and the ratio of luminosities

Given that the components are of a similar spectral class, we used calibrations for single stars to find the first approximation to their effective temperature and surface gravity. Following Kurucz (1995) we found $T_{\rm eff} = 7350$K, $\log g = 3.7$ using *UBV* colors and $T_{\rm eff} = 7200$K, $\log g = 4.0$ using *uvby* colors. So we selected the nearest root in the Kurucz (1995) grid of atmosphere models: the model with $T_{\rm eff} = 7250$K, $\log g = 4.0$ with solar chemical composition and a microturbulent velocity of 2.0 km s^{-1}. Then, we calculated a synthetic spectrum for the whole observed region. Two copies of this spectrum were shifted in accordance with the observed radial velocities of the

Table 2. Orbital elements of HD 153720 .

Element	Units	Heard & Hurkens (1975)		First solution		Second solution	
		Value	Error	Value	Error	Value	Error
P	days	11.01147	0.00007	11.01160	0.00009	11.01161	0.00006
γ	km s^{-1}	−13.6	0.1	−13.0	0.2	−13.5	0.1
K_1	km s^{-1}	72.5	0.2	71.5	0.5	72.3	0.3
K_2	km s^{-1}	73.2	0.2	74.1	0.5	73.3	0.3
e		0.389	0.002	0.390	0.004	0.389	0.003
ω	degrees	306.3	0.3	306.3	0.7	306.3	0.5
T_0	J.D.	2 441 018.702	0.010	2 441 018.694	0.022	2 441 018.694	0.014
$M_A \sin^3 i$	$M_\odot$	1.38	0.01	1.40	0.02	1.38	0.01
$M_B \sin^3 i$	$M_\odot$	1.37	0.01	1.35	0.02	1.37	0.01
M_A/M_B		1.01		1.04		1.01	

components and coadded with the assumption that L_A/L_B = 1.0. The composite synthetic spectrum was used for continuum placement and line identification.

To find more precise values of the components' parameters we used calculations of iron abundances obtained with different atmosphere models. This method was described in detail by Yushchenko et al. (1999), Yushchenko et al. (2004) and Gopka et al. (2004). Briefly, we calculate the iron abundance from individual lines for each point across a four-dimensional grid involving $T_{\rm eff}$, log g, $v_{\rm micro}$, and L_A/L_B. For each grid point, the coefficients of correlations between the equivalent widths (and the excitation potentials) and the iron abundances, and the scatter of the abundances were calculated. On the assumption that L_A/L_B = 1, the correct atmosphere parameters were selected as those providing zero (or very close to zero) correlation coefficients and minimal scatter in the derived iron abundances.

Next, we interpolated in the Kurucz (1995) grid to construct a mini-grid with effective temperatures 6750 K $\le T_{\rm eff} \le$ 7750 K ($\Delta T_{\rm eff}$ = 25 K) and surface gravities from 3.5 $\le$ log $g \le$ 4.5 (Δlog g = 0.1). 54 lines of neutral iron in the spectrum of the primary and 44 lines in the spectrum of secondary were used for the calculations. These clean lines were selected from synthetic spectra of the components. Solar oscillator strengths of these lines were found using the Liège solar atlas (Delbouille et al. 1974), as described below in the section on abundance analysis. Calculations of iron abundances from neutral iron lines were made for all the above listed models with different microturbulent velocities ($0.5 \le v_{\rm micro} \le 8.0$) and light ratio of the components ($0.85 \le L_A/L_B \le 1.15$). The Kurucz (1995) WIDTH9 program was used.

The best set of parameters are $T_{{\rm eff}\,A}$ = 7425 ± 50 K, log g_A = 4.0 ± 0.15, $v_{{\rm micro}\,A}$ = 2.7 ± 0.2 km s^{-1} for component A, and $T_{{\rm eff}\,B}$ = 7125 ± 50 K, log g_B = 3.9 ± 0.15, $v_{{\rm micro}\,B}$ = 2.7 ± 0.2 km s^{-1}, for component B. The ratio of luminosities is L_A/L_B = 1.10 ± 0.025. The errors are internal errors. High dispersion spectra permit us to use unblended iron lines of the components to find the atmosphere parameters. That is why the errors are of the same order as those found for single or SB1 stars; see, for example, our analyses of the barium star HD 202109 (Yushchenko et al. 2004) or the metal-poor halo star HD 221170 (Gopka et al. 2004). Of course, larger systematic errors can exist, and these errors will influence determinations of the parameters of both single and double stars.

The above-listed parameters were used for the abundance determinations. The ratio of luminosities was assumed to be 1.10 at wavelength 5800 Å. For other wavelengths it was changed in accordance with the ratios of the Kurucz (1995) predicted fluxes interpolated to the above mentioned parameters. All abundance calculations, except for the neutral iron lines, were made using the spectrum synthesis method. In this method it is necessary to know the line broadening parameters. In our case these parameters are the velocities of rotation and macroturbulence.

5. Synchronization of rotation, age and mass of HD 153720

We estimate the projected rotational velocity by analyzing the profiles of iron lines with accurate oscillator strengths. We find that $v \sin i$ = 15 km s^{-1} for both components. This value includes all possible line broadening mechanisms, including macroturbulence. The following argument shows that our estimate of the projected rotational velocity is a plausible value.

The Hipparcos parallax of HD 153720 is 10.56 ± 0.50 mas. Taking into account the visual magnitude of HD 153720, the bolometric corrections from Kurucz (1995), our parameters of atmosphere models and the flux ratio of the components, we find the radii of the components to be R_A = 1.86 $R_\odot$, and R_B = 1.92 $R_\odot$ and their luminosities to be L_A = 9.54 $L_\odot$ and L_B = 8.55 $L_\odot$. Given the radius and the $v \sin i$ = 15 km s^{-1}, we may estimate an upper limit to the period of rotation for a component: the upper limits are $6\overset{\rm d}{.}3$ and $6\overset{\rm d}{.}5$ for components A and B, respectively. These estimates are approximately half the orbital period.

Synchronization of orbital and rotational velocities requires that the components rotate with velocities near $v_{\rm circle}$ = 8.5–9 km s^{-1} in the case of a circular orbit. The eccentricity of the orbit is near 0.4. The maximum orbital velocity with this

value of the eccentricity is approximately 50 percent higher than the mean orbital velocity. Tidal effects are strongest when the distance between stars is smallest, i.e., at maximum orbital velocity. Then, we expect that, at synchronization, the rotational velocities of the components will be higher than the values for circular orbits. The values of the pseudosynchronized velocity for an elliptical orbit can be calculated using the formula of Giuricin et al. (1984):

$$v = v_{\rm circle}(1+e)^{1/2}/(1-e)^{3/2}. \quad (1)$$

For our case, this formula gives a result near 22 km s^{-1}. For an inclination of the orbit i near 43 degrees, this corresponds to the observed $v \sin i$ of 15 km s^{-1} for both components. Then, the masses of the components are larger than 2.0 $M_\odot$.

However, evolutionary tracks (Claret 1995; Claret & Gimenez 1995; Claret 1997; Claret & Gimenez 1998) predict that a 2.0 $M_\odot$ star at the observed temperature and surface gravity has twice the observed luminosity. The evolutionary tracks show that the masses of the components are in the range 1.48−1.65 $M_\odot$ and the age in the range 1.5−1.7 × 10^9 years. At these lower masses, the angle i is the range 70 to 78 degrees and the rotational velocities of the components are near 16 km s^{-1}. These velocities of the components of HD 153720 are slower than the pseudosynchronized velocity. The difference between the predicted pseudosynchronized velocity (22 km s^{-1}) and the observed value is in the range of scattering of observed values for different binary systems investigated by Giuricin et al. (1984).

Note that from the Hipparcos-based diameters and spectroscopic surface gravities log g_A = 4.0, log g_B = 3.9 we find the masses of the stars to be M_A = 1.27 $M_\odot$ and M_B = 1.07 $M_\odot$, values lower than from the evolutionary tracks. To remove this discrepancy we should increase the spectroscopic surface gravities to the values log g_A = 4.07−4.12, log g_B = 4.04−4.09. These differences are within the errors of our determinations of the spectroscopic surface gravities of the components.

6. Abundance analysis

We calculated the abundances of all elements except iron by using synthetic spectra, as described in detail by Yushchenko et al. (2004). The synthetic spectra of the components were constructed using the SYNTHE code of Kurucz (1995) and the URAN code (Yushchenko 1998). We used atomic lines from the following databases: Kurucz (1995), Morton (2000), DREAM (Biemont et al. 2002) and VALD (Piskunov et al. 1995) with a few lines from other sources. We took into account the hyperfine structure and isotopic splitting of Mn, Cu, and Ba lines, as given by Kurucz (1995) and François (1996). The synthetic spectra of the components were shifted to the observed radial velocities and coadded, taking into account the flux ratio of the components. The value L_A/L_B = 1.1 was used for the wavelength of 5800 Å. For other wavelengths the flux ratio was scaled according to theoretical fluxes from the Kurucz (1995) models. To find unblended lines we compared the observed spectrum with the coadded synthetic spectrum of the system. To find the uncertainties of the derived abundances we made calculations for each component with two atmosphere models – that of the component and that of the other component. This procedure permits us to estimate the uncertainties due to the atmosphere model and due to the fitting method. The data for the individual lines can be found on the web sites "users.odessa.net/~yua" and "yushchenko.netfirms.com". In Figs. 1 and 2, we present a part of the observed spectrum of HD 153720 , the synthetic spectra of the components and the coadded synthetic spectrum.

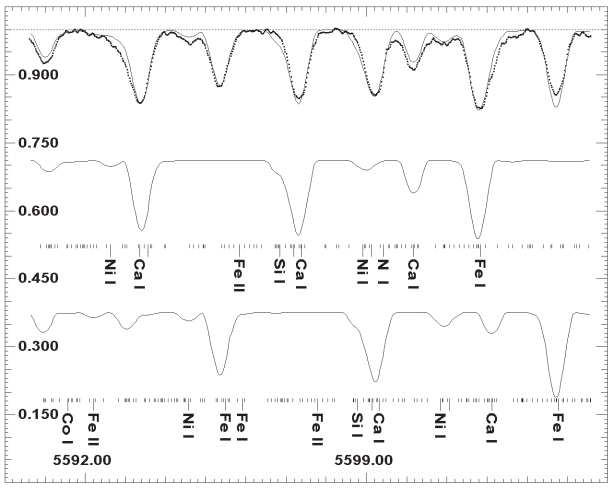

Fig. 1. Part of the spectrum of HD 153720 . The axes are the wavelength in angstroms and relative flux. In the top part of the figure the points are the observed spectrum. The solid line is the sum of the synthetic spectra of the components. Scaled synthetic spectrum of the component A is shown separately in the middle part, of the component B – in the bottom part of the figure. Synthetic spectra of the components are shifted in accordance with the observed radial velocities and smoothed by instrumental and rotational profiles. The positions of the spectral lines, which were taken into account in synthetic spectra calculations are marked by short and long dashes (faint and strong lines). Some strong lines are identificated.

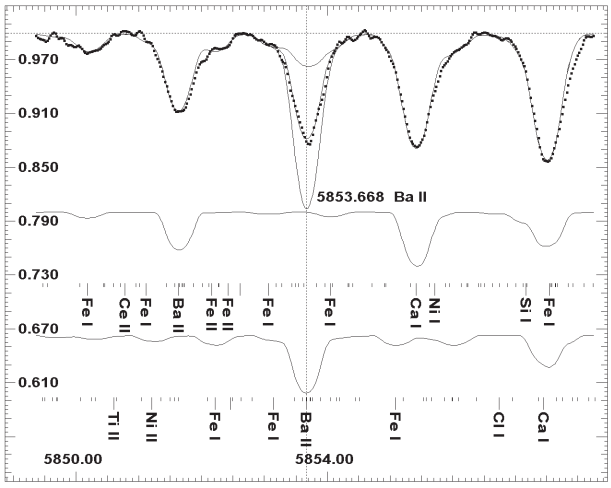

Fig. 2. The same as Fig. 1 in the vicinity of the Ba II line λ5853.688. The position of this line in the spectrum of component B is marked by a vertical broken line. Three coadded synthetic spectra near the position of bariun lines in component B correspond to the best barium abundance, and the abundances changed by ±0.5 dex with respect to the best abundance.

Table 3. Chemical composition of HD 153720 .

Z	Elem.	A–⊙	σ	N	B–⊙	σ	N	A–⊙	σ	B–⊙	σ
								Model B		Model A	
1	2	3	4	5	6	7	8	9	10	11	12
6	C I	−0.37	0.09	4	−0.40	0.08	4	−0.31	0.10	−0.52	0.10
7	N I	−0.31	0.01	2	−0.52	0.23	2	−0.03	0.12	−0.52	0.12
8	O I	−0.19		1	−0.48	0.19	2	−0.05		−0.66	0.22
11	Na I	−0.16	0.02	2	0.16	0.18	3	−0.15	0.05	0.27	0.21
12	Mg I	−0.16	0.19	2	−0.37	0.12	4	−0.23	0.20	−0.29	0.09
	Mg II				−0.21		1			−0.37	
13	Al I	−0.09	0.15	2	−0.09	0.07	3	−0.16	0.19	−0.03	0.09
14	Si I	−0.11	0.10	5	−0.14	0.07	6	−0.17	0.11	−0.07	0.07
	Si II	−0.09		1	−0.14		1	0.05		−0.25	
16	S I	0.23	0.10	6	0.15	0.07	6	0.25	0.10	0.11	0.06
19	K I	0.09	0.11	2	0.17		1	0.09	0.22	0.31	
20	Ca I	−0.17	0.16	11	−0.49	0.12	10	−0.27	0.15	−0.39	0.15
	Ca II	−0.19		1	−0.47		1	−0.08		−0.65	
21	Sc II	−0.03	0.07	4	−0.47	0.04	4	−0.16	0.09	−0.34	0.09
22	Ti I	0.18	0.07	2	−0.23	0.05	2	−0.02	0.12	−0.05	0.03
	Ti II	−0.14	0.13	8	−0.37	0.10	4	−0.23	0.13	−0.27	0.07
24	Cr I	−0.08	0.09	6	−0.01	0.09	7	−0.22	0.09	0.12	0.08
	Cr II	−0.21	0.09	7	−0.07	0.02	8	−0.25	0.09	−0.05	0.04
25	Mn I	0.00	0.08	4	0.03	0.03	4	−0.09	0.09	0.15	0.03
26	Fe I	−0.03	0.11	54	+0.02	0.14	44	−0.14	0.11	0.13	0.14
	Fe II	+0.04	0.13	8	+0.14	0.10	10	0.00	0.13	0.15	0.10
28	Ni I	−0.07	0.13	18	0.01	0.12	21	−0.18	0.13	0.13	0.11
29	Cu I				0.05	0.06	2			0.14	0.05
30	Zn I	0.11	0.10	2	0.22		1	0.00	0.11	0.33	
39	Y II	0.36	0.08	4	0.53	0.10	3	0.23	0.07	0.60	0.22
40	Zr II	0.21	0.10	2	0.23		1	0.10	0.04	0.25	
56	Ba II	0.23	0.12	3	0.37	0.11	2	0.06	0.15	0.48	0.04
58	Ce II	0.19		1				0.10			

We also derived the solar abundances from the adopted lines. For this calculation, we use the Liège Solar Atlas (Delbouille et al. 1974) and the Grevesse & Sauval (1998) model atmosphere. The adopted values of the microturbulent and macroturbulent velocities are 0.8 km s^{-1} and 1.8 km s^{-1} respectively. The continuum in the Liège Solar atlas is corrected in accordance with Ardeberg & Virdefors (1979) and Rutten & van der Zalm (1984). The solar abundances are used with the stellar abundances to obtain the differential abundances which are independent of the adopted oscillator strengths.

Mean results for the investigated elements are listed in Table 3. The first columns in Table 3 are from left to right the atomic number, and the identification of atom or ion. Then follow four entries, two of three columns and two of two columns, concerning the abundances: the three columns are the mean logarithmic abundance of the element relative to the solar value, the rms error of one measurement and the number of lines contributing to the mean abundance. The first two of the four entries concern results for components *A* and *B* obtained with the model atmosphere of that component. The last two entries, each of two columns, give the abundances and the rms error of each component when analysed with the model atmosphere of the other component.

Figure 3 shows the abundances versus atomic number. The abundance patterns are those of metallic line stars. C, N, O, Mg, Al, Si, and Ca are underabundant with respect to the Sun. Cu and heavier elements are overabundant in both components. The abundances of other elements are approximately solar values or different for the *A* and *B* components. Both components of HD 153720 are metallic line stars.

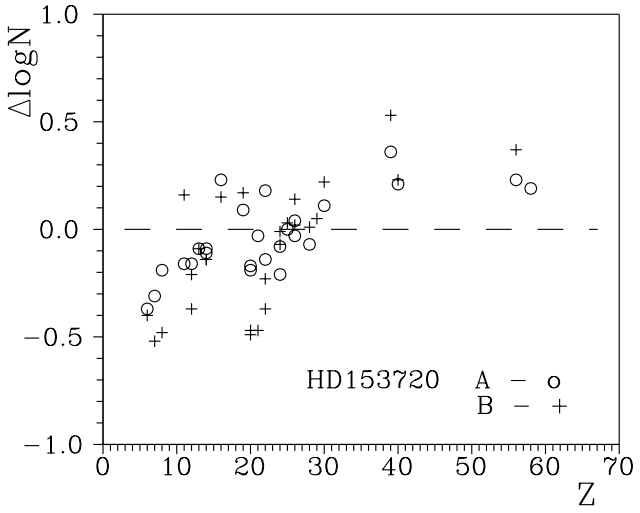

Fig. 3. The abundances of chemical elements in the atmosphere of HD 153720 *A* and *B* with respect to their abundances in the solar atmosphere.

7. Normal A stars are rare

The metallic line (Am) stars were first recognized as a group by Titus & Morgan (1940). They found that the Ca K line did not lead to the same spectral classification as the hydrogen lines for some Hyades A stars. Since then, it has been noticed that most if not all slowly rotating A and F stars exhibit abundance anomalies. The abundances of CNO are generally below solar, while those of iron- peak elements are generally above solar, and the species in between can be either under- or overabundant.

The classical Am stars are characterized by a general enhancement of the metallic lines but a marked weakness of the lines of Ca and Sc when compared to normal A stars at the resolution of classification spectra. Lines of heavy elements are enhanced for most stars. The AmFm stars may arise as a result of radiatively driven diffusion processes (Michaud 1970). Binarity is a common feature of Am stars (Abt 1961) and tidal effects might be of great importance in controlling diffusion processes (Budaj 1996). The general catalog of Am and Ap stars (Renson et al. 1991) contains 6684 objects but only for a small number of these stars have chemical abundances been determined from high resolution spectra.

It should be noted that Am and other chemically peculiar stars are significantly more common than normal A stars. It is very hard to find a star with a normal (solar-like) chemical composition among A-type stars. Nonetheless, Budaj (1996) compiled a list of 61 apparently non-chemically peculiar binaries with spectral classes from A4 to F1.

Eight of Budaj's stars including HD 153720 have been analysed for their composition. For six of the eight, abundance anomalies indicative of chemical peculiarities have been seen in one or both components of these binaries: the six stars are comprised of HD 28910 (86 Tau – Varenne & Monier 1999; and Takeda & Sadakane 1997), HD 83808 (*o* Leo – Griffin 2002), HD 153720 (this paper), HD 178449 (Budaj & Iliev 2003), HD 205767 and HD 217792 (Erspamer & North 2003). Two stars, HD 32537 (9 Aqr – Hui-Bon-Hoa 2000) and R CMa (Tomkin & Lambert 1989) have been classified as normal, but it should be noted that the abundances of only six and five chemical elements were measured for HD 32537 and R CMa, respectively and, furthermore, the heaviest investigated element was Ni. If the abundances of heavier elements are measured, it is possible that the classification of the stars would be changed. Continued scrutiny of Budaj's binaries may uncover systems without chemical peculiarities but it is clear that it is difficult to find a normal star in this region of HR diagram.

8. Conclusion

In this paper, we present the first abundance analysis of the components of the SB2 system HD 153720 . The atmospheric parameters of the components were found from careful analysis of iron abundances calculated from individual atomic lines. We used differential spectrum synthesis to find the abundances of 21 elements in both components. In addition, Cu was found only in component *A*, and Ce – only in component *B*.

HD 153720 is a system with twin metallic-line (Fm) components. The star has not been classified previously as a metallic line star.

The Hipparcos parallax and our parameters of atmosphere models enable us to estimate the mass and the age of the components, and the inclination of the orbit. The rotational velocities of the components are probably slightly lower than the pseudosynchronized velocity.

There is a hint that this spectroscopic binary may have a third body. Our radial velocities are offset by 4 km s^{-1} from the published data obtained about thirty years earlier.

The star HD 153720 highlights the difficulty of finding normal A-type stars as members of a spectroscopic binary. It appears in Budaj's (1996) list of such normal spectroscopic binaries, but our abundance analysis reveals chemical peculiarities characteristic of metallic line stars.

Acknowledgements. We would like to thank to L. Delbouille and G. Roland for sending us the Liège Solar Atlas. We thank V. Woolf for assistance with reduction of the McDonald spectra. We use data from NASA ADS, SIMBAD, CADC, VALD, NIST, and DREAM databases and we thank the teams and administrators of these projects.
Work by A.Y. and Y.K. was supported by the Astrophysical Research Center for the Structure and Evolution of the Cosmos (ARCSEC) of Korea Science and Engineering Foundation (KOSEF) through the Science Research Center (SRC) program.

References

Abt, H. 1961, ApJS, 6, 37
Adelman, S., Ryabchikova, T., & Davydova, E. 1998, MNRAS, 297, 1
Ardeberg, A., & Virdefors, B. 1979, A&AS, 36, 317
Biémont, J., Palmeri, P., & Quinet, P. 2002, Database of rare earths at Mons University, `http://www.umh.ac.be/~astro/dream.html`
Budaj, J. 1996, A&A, 313, 523
Budaj, J., & Iliev, I. K. 2003, MNRAS, 346, 27
Catanzaro, G., Leone, F., & Leto, P. 2003, A&A, 407, 669

Claret, A. 1995, A&AS, 108, 441
Claret, A. 1997, A&AS, 125, 439
Claret, A., & Gimenez, A. 1995, A&AS, 114, 549
Claret, A., & Gimenez, A. 1998, A&AS, 133, 123
Delbouille, L., Roland, G., & Neven, L. 1973, Photometric Atlas of the Solar Spectrum from λ3000 to λ10 000, Liège, Institut d'Astrophysique de l'Université de Liège
Erspamer, D., & North, P. 2003, A&A, 398, 1121
Fekel, F. C., & Tomkin, J. 1993, AJ, 106, 1156
François, P. 1996, A&A, 313, 229
Gopka, V. F., Yushchenko, A. V., Mishenina, T. V., et al. 2004, Astronomy Reports, accepted
Giuricin, G., Mardirossian, F., & Mezzetti, M. 1984, A&A, 135, 393
Griffin, R. E. M. 2002, AJ, 123, 988
Grevesse, N., & Sauval, A. J. 1998, Space Sci. Rev., 85, 161
Heard, J., & Hurkens, R. 1975, JRASC, 69, 25
Hui-Bon-Hoa, A. 2000, A&AS, 144, 203
Khokhlova, V. L., Zverko, Yu., Ziznovskij, I., & Griffin, R. E. M. 1995, Astron. Lett., 21, 818
Kurucz, R. L. 1995, ASP Conf. Ser., 81, 583
Michaud, G. 1970, ApJ, 160, 641
Morton, D. C. 2000, ApJS, 130, 403
Moshir, M., Kopan, G., Conrow, T., et al. 1989, The IRAS Faint Source Survey Version 2.0 (ADC CD-ROM 1, 1991)
Piskunov, N., Kupka, F., Ryabchikova, T., Weiss, W., & Jeffery, C. 1995, A&AS, 112, 525
Renson, P., Gerbaldi, M., & Catalano, F. A. 1991, A&AS, 1991, 89, 429
Rutten, R. J., & van der Zalm, E. B. J. 1984, A&AS, 55, 143
Scarfe, C. D., Barlow, D. J., Fekel, F. C., et al. 1994, AJ, 107, 1529
Takeda, Y., & Sadakane, K. 1997, PASJ, 49, 367
Thompson, G. I., Nandy, K., Jamar, C., et al. 1978, Catalogue of Stellar Ultraviolet Fluxes, ADC CD-ROM 1, 1991
Titus, J., & Morgan, W. W. 1940, 92, 256
Tomkin, J., & Lambert, D. L. 1989, MNRAS, 241, 777
Tsymbal, V. V., Kotchukhov, O. P., Khokhlova, V. L., & Lambert, D. L. 1998, Astron. Lett., 24, 90
Tull, R. G., MacQueen, P. J., Sneden, C., & Lambert, D. L. 1995, PASP, 107, 251
Varenne, O., & Monier, R. 1999, A&A, 351, 247
Young, A. 1976, PASP, 88, 275
Young, R. K. 1942, Publ. David Dunlap Obs., 1, 251
Yushchenko, A. V. 1998, Proc. of the 29th Conf. of variable star research, Brno, Czech Republic, November 5−9, 201
Yushchenko, A. V., Gopka, V. F., Khokhlova, V. L., Musaev, F. A., & Bikmaev, I. F. 1999, Astron. Lett., 25, 453
Yushchenko, A., Gopka, V., Kim, C., et al. 2002, J. Korean Astron. Soc., 35, 209
Yushchenko, A., Gopka, V., Khokhlova, V., & Tomkin, J. 2001, IBVS, 5213
Yushchenko, A. V., Gopka, V. F., Kim, C., et al. 2004, A&A, 413, 1105

Online Material

Table 4. Iron lines in the spectrum of HD 153720.

λ (Å)	Eq. width		Abundances		Oscillator strengths			Radial velocities	
	A	B	A	B	Kurucz	Solar	Hirata	A	B
1	2	3	4	5	6	7	8	9	10
Fe I lines									
4187.038	62				−0.548	−0.328	−0.51	−59.965	
4219.360		66			0.120	0.136	0.12		43.874
4267.826	28		7.603		−1.110	−1.495	−1.17	−59.251	
4271.153		95			−0.349	−0.233	−0.349		45.658
4547.846	37		7.536		−0.780	−0.889	−1.01		
4602.940		62			−1.950	−2.247	−2.21		46.731
4625.044	35		7.607		−1.340	−1.251	−1.34	−60.055	
4643.463	18	26	7.449	7.656	−1.290	−1.259	−1.15	−57.428	46.129
4678.845	50		7.732		−0.660	−0.706	−0.83	−58.852	
4962.565	15	15	7.757	7.718	−1.290	−1.297	−1.18	−58.266	
4966.087	52		7.591		−0.890	−0.733	−0.87	−59.492	
4973.101		35		7.864	−0.950	−0.982	−0.95		45.001
4994.129	30	40	7.570	7.728	−3.080	−3.165	−2.956	−59.278	43.851
5044.210		25		7.797	−2.150	−2.089	−2.02		
5068.765		56		7.868	−1.230	−1.139	−1.04		46.340
5133.681		66			0.140	0.670	0.14		44.586
5159.050	28		7.722		−0.820	−0.795	−0.82	−58.545	
5162.292		78			0.020	0.222	0.02		44.339
5165.407	35		7.559		−0.035	−0.506	−0.035	−58.764	
5171.595	65				−1.793	−1.869	−1.793	−59.737	
5187.914		10		7.524	−1.260	−1.359	−1.37		43.542
5191.455	61				−0.656	−0.397	−0.55	−57.833	
5192.343	69	71			−0.521	−0.276	−0.42	−58.343	45.641
5215.179	52		7.603		−0.933	−0.809	−0.933	−57.168	
5216.274	55		7.842		−2.150	−2.256	−2.150	−58.420	
5217.389		42		7.527	−1.097	−1.051	−1.07		45.594
5232.939	89				−0.190	0.207	−0.06	−59.495	
5242.491	39	42	7.659	7.751	−0.840	−0.934	−0.97	−59.729	44.690
5250.645		40		7.682	−2.050	−2.081	−2.18		45.934
5269.537	100	100			−1.321	−1.340	−1.321	−59.025	44.460
5302.299	68	67			−0.880	−0.682	−0.720	−58.321	44.977
5324.178	93				−0.240	0.122	−0.103	−60.277	
5339.928		58		7.574	−0.680	−0.547	−0.647		44.211
5364.858		60		7.602	0.220	0.410	0.23		
5383.369	82	77			0.500	0.877	0.64	−59.893	44.912
5393.167		60		7.688	−0.910	−0.626	−0.715		46.109
5397.127	82	77			−1.993	−2.231	−1.993	−58.962	45.187
5424.069	93	87			0.520	1.002	0.52	−59.941	44.686
5445.042	54		7.372		−0.020	0.264	−0.02	−58.829	
5470.092		4		7.642	−1.810	−1.701	−1.701		
5473.900	28		7.533		−0.760	−0.714	−0.700	−58.190	
5483.098		12		7.741	−1.580	−1.483	−1.41		
5501.464	42		7.775		−2.950	−3.071	−3.05	−58.226	
5506.778	45		7.680		−2.797	−2.867	−2.797	−57.788	
5569.618		58		7.394	−0.540	−0.263	−0.54		44.649
5576.090	48		7.488		−1.000	−0.704	−1.00	−59.221	
5618.631	12		7.688		−1.380	−1.337	−1.28		
5619.587		7		7.750	−1.700	−1.591	−1.70		
5638.262		21		7.395	−0.870	−0.746	−0.87		45.115
5679.025	15		7.566		−0.920	−0.766	−0.92	−60.048	

Table 4. continued.

λ (Å)	Eq. width		Abundances		Oscillator strengths			Radial velocities	
	A	B	A	B	Kurucz	Solar	Hirata	A	B
1	2	3	4	5	6	7	8	9	10
5731.762	12		7.515		−1.300	−1.137	−1.30	−58.187	
5752.023	15		7.657		−1.267	−0.945	−1.00	−59.390	
5775.080	17	21	7.701	7.802	−1.203	−1.160	−1.30	−60.450	45.915
5862.353	38	39	7.700	7.753	−0.058	−0.347	−0.36	−59.141	44.362
5883.813		16		7.588	−1.360	−1.323	−1.36		44.965
5905.689	12	16	7.469	7.607	−0.730	−0.800	−0.87		
5934.653	19		7.573		−1.170	−1.189	−1.17	−58.219	
5987.066		29		7.845	−0.556	−0.507	−0.507		
6008.554	23		7.409		−1.078	−0.945	−0.97		
6055.992		31		7.718	−0.460	−0.381	−0.46		46.013
6065.482	48	51	7.559	7.633	−1.530	−1.430	−1.41	−59.335	45.101
6078.491	34	37	7.768	7.874	−0.424	−0.309	−0.38		46.188
6093.666		7		7.749	−1.500	−1.433	−1.451		
6136.615	57		7.626		−1.400	−1.375	−1.40	−57.915	
6137.694	51	47	7.479	7.353	−1.403	−1.291	−1.35	−58.882	44.766
6165.361		9		7.603	−1.550	−1.516	−1.47		44.808
6170.504	27		7.664		−0.440	−0.391	−0.44		
6180.203	8.5	8.5	7.715	7.618	−2.780	−2.692	−2.596		44.652
6191.558	50	60	7.459	7.757	−1.600	−1.424	−1.42	−60.887	
6200.314	10	16	7.395	7.552	−2.437	−2.382	−2.37	−58.867	45.377
6213.429	17		7.595		−2.660	−2.587	−2.48	−58.019	
6219.279	21		7.528		−2.433	−2.422	−2.433	−58.880	
6246.317		44		7.497	−0.960	−0.704	−0.733		45.283
6252.554	45		7.555		−1.687	−1.674	−1.687	−58.615	
6265.131	20	23	7.602	7.586	−2.550	−2.539	−2.54	−57.971	45.482
6301.498	52		7.661		−0.745	−0.616	−0.59	−58.160	
6302.494		30		7.602	−1.203	−1.130	−1.203	−58.103	45.165
6335.328	33	45	7.639	7.888	−2.230	−2.217	−2.18	−58.701	
6336.823	50		7.770		−1.050	−0.761	−0.78	−56.369	
6393.602	51	52	7.633	7.642	−1.620	−1.579	−1.58	−58.869	44.943
6400.000		64			−0.520	−0.082	−0.29		45.460
6411.647	46	50	7.349	7.474	−0.820	−0.469	−0.595	−59.311	45.191
6421.349	36	44	7.587	7.734	−2.027	−2.034	−2.027	−58.288	46.103
6430.844	40		7.581		−2.006	−2.006	−2.006	−59.554	
6677.989	50		7.533		−1.470	−1.311	−1.42	−59.190	
6750.150	15		7.603		−2.621	−2.527	−2.608	−57.625	
6810.257	13	16	7.702	7.784	−1.120	−1.044	−0.99		43.250
7411.154		35		7.343	−0.428	−0.303	−0.25		45.406
7491.649	20		7.706		−1.014	−1.039	−0.86	−59.565	
7495.060	60	60	7.551	7.583	−0.102	0.106	0.23	−58.898	45.098
7511.015	64	70			0.107	0.338	0.33	−58.892	44.922
7710.360	17	17	7.624	7.566	−1.051	−1.118	−1.11	−58.342	
7807.952	17		7.679		−0.697	−0.600	−0.697	−60.953	
8085.176	48	42	7.651	7.489	−0.240	−0.149	−0.37	−59.160	45.106
8824.216	79	77			−1.364	−1.476	−1.54	−59.878	44.930
Fe II lines									
4508.288		84			−2.210	−2.613	−2.58		
4515.339	85	80			−2.480	−2.700	−2.48		
4520.224	75	73			−2.600	−2.946	−2.98		
4541.524		57		7.733	−3.050	−3.229	−3.05		

Table 4. continued.

λ (Å)	Eq. width		Abundances		Oscillator strengths			Radial velocities	
	A	B	A	B	Kurucz	Solar	Hirata	A	B
1	2	3	4	5	6	7	8	9	10
4576.340		64			−3.040	−3.239	−2.94		
4635.316		26		7.797	−1.650	−1.729	−1.65		
5197.577		80			−2.100	−2.401	−2.116		
5362.869	80				−2.739	−2.773	−2.739		
5414.073	31	32	7.864	7.942	−3.790	−3.806	−3.58		
5425.257	45	43	7.761	7.797	−3.360	−3.499	−3.36		
5534.847		64			−2.930	−3.009	−2.996		
5991.376	33	33	7.613	7.657	−3.557	−3.811	−3.74		
6084.111	22		7.608		−3.808	−4.031	−3.808		
6147.741	44		7.613		−2.721	−2.950	−2.72		
6149.258	49		7.730		−2.724	−2.961	−2.92		
6179.384		9		7.768	−2.602	−2.774	−2.81		
6247.557		60		7.780	−2.329	−2.560	−2.51		
6248.898		10		7.878	−2.696	−2.859	−2.696		
6385.451		10		7.828	−2.618	−2.841	−2.618		
7479.693	10		7.444		−3.588	−3.924	−3.88		
7515.831		16		7.568	−3.432	−3.626	−3.53		
7711.723	57		7.701		−2.543	−2.780	−2.74		

Column 1. Wavelengths (Å).
Column 2. Equivalent widths of the lines in mÅ. Component A.
Column 3. Equivalent widths of the lines in mÅ. Component B.
Column 4. Abundances in the scale $\log N(\mathrm{H}) = 12$. Component A.
Column 5. Abundances in the scale $\log N(\mathrm{H}) = 12$. Component B.
Remark: only lines with eq. widths <60 mÅ were used for abundance determinations.
Column 6. Oscillator strengths from Kurucz database.
Column 7. Oscillator strengths calculated from Solar spectrum.
Column 8. Oscillator strengths from Hirata catalogue (VI/68 in CDS).
Column 9. Radial velocities in km s^{-1}. Component A.
Column 10. Radial velocities in km s^{-1}. Component B.

Table 5. Lines of other elements in the spectrum of HD 153720.

λ (Å)	Code	Eq. width		log gf	Sun		Comp. A		Comp. B		A	B
		A	B		$\Delta\log gf$	%	$\Delta\log N$	%	$\Delta\log N$	%	mod B	mod A
1	2	3	4	5	6	7	8	9	10	11	12	13
4775.897	6.00	25	22	−2.16	0.14	99	−0.52	98	−0.50	100	−0.49	−0.64
5052.167	6.00	40	35	−1.65	0.21	99	−0.31	100	−0.44	99	−0.23	−0.57
5380.337	6.00	28	20	−1.84	0.12	98	−0.32	99			−0.26	
7111.472	6.00		13	−0.81	−0.44	97			−0.29	100		−0.37
7115.172	6.00	30	22	−0.71	−0.32	91			−0.37	95		−0.49
7837.095	6.00	6		−1.46	−0.18	75	−0.33	96			−0.26	
7468.312	7.00	10.5	10	−0.27			−0.30	100	−0.29	100	−0.15	−0.40
8711.703	7.00	12	8	−0.38			−0.31	88	−0.76	93	+0.10	−0.64
6155.971	8.00			−1.05			−0.19	50			−0.05	
6156.778	8.00			−0.73	0.19	64			−0.66	46		−0.89
6158.187	8.00			−0.44	0.01	77			−0.29	44		−0.44
5682.633	11.00	40		−0.70	0.09	100	−0.17	100			−0.10	
5688.205	11.00	75	70	−0.45	0.22	99	−0.14	98	−0.09	98	−0.20	−0.02
8183.255	11.00		104	0.23					0.22	100		+0.34
8194.824	11.00		128	0.49					0.35	99		+0.48
4702.990	12.00	140	115	−0.70			0.03	100	−0.22	99	−0.02	−0.16
5172.684	12.00	170	140	−0.40			−0.35	100	−0.48	100	−0.43	−0.36
5528.405	12.00		90	−0.62					−0.28	100		−0.24
5711.088	12.00		17	−1.83	0.04	100			−0.49	100		−0.39
7877.054	12.01		30	0.39	0.01	99			−0.21	100		−0.37
6696.023	13.00	11	11	−1.35	−0.25	94	−0.24	69	−0.14	77	−0.35	+0.01
7835.309	13.00		10	−0.65	−0.06	100			−0.14			−0.16
7836.134	13.00	17	16	−0.49	−0.10	100	0.06	100	0.00	100	+0.02	+0.05
5645.613	14.00		10	−2.14	+0.07	100			−0.11	99		+0.00
5690.425	14.00		11	−1.87	+0.04	100			−0.07	97		+0.01
5708.400	14.00	35	30	−1.47	+0.07	100			−0.27	99		−0.18
6976.513	14.00	13		−1.17	+0.20	99	−0.21	99			−0.28	
7405.772	14.00	30	40	−0.82	+0.20	99	−0.12	100	−0.20	100	−0.19	−0.15
7423.496	14.00	34		−0.31	−0.19	100	−0.23	100			−0.29	
7680.266	14.00	37	36	−0.69	+0.10	100	−0.05	99	−0.10	100	−0.11	−0.04
7742.717	14.00	46	50	−0.69	+0.18	96	0.04	96	−0.09	96	+0.01	−0.06
6371.371	14.01	79	66	0.00	−0.16	100	−0.09	100	−0.14	100	+0.05	−0.25
4694.113	16.00	25	17	−1.77	−0.07	89	0.41	99	0.08	97	+0.40	+0.10
6045.991	16.00	18	18	−1.24	+0.00	51	0.10	46	0.08	47	+0.15	+0.07
6052.674	16.00	19	24	−0.74	−0.18	99	0.20	94	0.22	94	+0.21	+0.21
6748.837	16.00	30	26	−0.60	−0.14	99	0.16	97	0.10	97	+0.18	+0.08
6757.171	16.00	34	33	−0.31	−0.20	100	0.23	99	0.24	99	+0.21	+0.16
8694.626	16.00	48	48	0.08	−0.23	99	0.25	99	0.19	99	+0.37	+0.05
7664.911	19.00	70		+0.13			−0.01	100			−0.14	
7698.974	19.00	68	65	−0.17			0.20	100	0.17	100	+0.31	+0.31

Table 5. continued.

λ (Å)	Code	Eq. width		log gf	Sun		Comp. A		Comp. B		A	B
		A	B		$\Delta\log gf$	%	$\Delta\log N$	%	$\Delta\log N$	%	mod B	mod A
1	2	3	4	5	6	7	8	9	10	11	12	13
4283.011	20.00	68	77	−0.29			−0.39	99			−0.49	
4318.652	20.00	110	80	−0.29	0.05	100	−0.43	99	−0.70	99	−0.46	−0.68
4435.679	20.00	105	84	−0.41	−0.04	100	−0.37	100	−0.43	100	−0.53	−0.32
4685.268	20.00		11	−0.54	−0.40	100			−0.25	92		−0.15
5581.965	20.00	39	30	−0.57	+0.06	100	−0.11	100	−0.54	100	−0.21	−0.44
5588.749	20.00		55	+0.31					−0.63	100		−0.56
5601.277	20.00	50		−0.55	+0.03	100	0.00	100			−0.09	
5857.451	20.00	74		+0.26	+0.02	100	−0.13	100			−0.21	
6162.173	20.00	90	65	−0.17			0.05	100	−0.45	100	−0.07	−0.27
6166.439	20.00	14		−1.16	+0.04	100	−0.01	100			−0.11	
6169.563	20.00	48	32	−0.27	+0.13	100	−0.15	99	−0.46	99	−0.25	−0.35
6439.075	20.00	92	73	0.39			−0.14	100	−0.53	100	−0.24	−0.41
6449.808	20.00	49	35	−1.01	+0.65	100	−0.22	100	−0.54	100	−0.32	−0.47
6499.650	20.00		21	−0.72	−0.06	100			−0.40	100		−0.29
8912.068	20.01	180	130	+0.57	+0.39	100	−0.19	100	−0.47	100	−0.08	−0.65
4400.389	21.01	90	55	−0.51	−0.09	100	−0.15	100	−0.48	100	−0.30	−0.29
5031.021	21.01	60	35	−0.26	−0.18	99	−0.01	99	−0.53	95	−0.16	−0.43
5239.813	21.01	33	24	−0.77	−0.03	100	0.00	99	−0.45	98	−0.09	−0.42
5526.790	21.01	77		+0.13	−0.09	100	0.04	100			−0.07	
5669.042	21.01		15	−1.12	+0.00	100			−0.41	94		−0.23
4534.778	22.00		23	+0.28	−0.23	100			−0.18	99		−0.02
4617.254	22.00	17		+0.39	−0.14	100	0.25	98			+0.10	
4999.504	22.00	30		+0.25	−0.34	100	0.11	98			−0.14	
6261.101	22.00		5	−0.48	−0.06	100			−0.27	82		−0.08
4312.864	22.01	86		−1.16			−0.37	100			−0.44	
4417.719	22.01	84	80	−1.43	+0.00	100	−0.27	100	−0.36	100	−0.38	−0.25
4421.938	22.01	38		−1.77	−0.07	95	0.08	100			+0.01	
4443.794	22.01		95	−0.70					−0.52	100		−0.39
4545.134	22.01	23		−1.87	−0.69	100	−0.17	99			−0.26	
4805.085	22.01	80		−1.10	+0.03	100	−0.07	100			−0.21	
5188.680	22.01	100	72	−1.21	−0.05	100	−0.11	100	−0.35	100	−0.19	−0.26
5211.536	22.01	20	17	−1.35	−0.20	100	−0.14	100	−0.24	100	−0.20	−0.19
6491.561	22.01	27		−1.79	−0.28	100	−0.07	98			−0.14	
4511.908	24.00		12	−0.34	−0.06	100			−0.10	92		+0.02
4646.148	24.00	34	35	−0.70	−0.26	100	−0.06	100	0.04	100	−0.18	+0.19
4651.282	24.00	24	19	−1.46	−0.08	100	0.05	100	−0.06	100	−0.12	+0.09
4652.152	24.00	24	33	−1.03	−0.19	100	0.02	100	−0.06	100	−0.16	+0.10
5296.691	24.00	19		−1.40			−0.23	100			−0.39	
5297.376	24.00	14	12	+0.17	−0.08	100	−0.13	100	−0.11	100	−0.23	+0.02
5787.965	24.00		14	−0.08	+0.01	100			0.09	100		+0.20
7400.226	24.00	12	15	−0.11	−0.01	100	−0.12	100	0.13	100	−0.24	+0.25
4554.988	24.01	35	33	−1.38	+0.00	100	−0.20	100	−0.05	99	−0.25	+0.00
4558.650	24.01	101		−0.66	+0.10	100	−0.27	100			−0.34	
4588.199	24.01	78		−0.63	−0.09	100	−0.35	100			−0.35	
4592.049	24.01	50	55	−1.22	−0.13	100	−0.23	99			−0.31	

Table 5. continued.

λ (Å)	Code	Eq. width		log gf	Sun		Comp. A		Comp. B		A	B
		A	B		$\Delta\log gf$	%	$\Delta\log N$	%	$\Delta\log N$	%	mod B	mod A
1	2	3	4	5	6	7	8	9	10	11	12	13
4616.629	24.01	40	43	−1.29	−0.13	100	−0.14	100	−0.07	100	−0.15	−0.10
4812.337	24.01		24	−1.80	−0.15	95			−0.11	99		−0.11
5237.329	24.01		55	−1.16	−0.10	100			−0.04	100		−0.07
5246.768	24.01	17	17	−2.45	+0.01	100	−0.03	100	−0.05	100	−0.08	−0.01
5308.408	24.01		24	−1.81	−0.11	98			−0.07	94		−0.01
5310.687	24.01	10	12	−2.28	+0.03	100			−0.09	100		−0.07
5313.563	24.01	37	36	−1.65	+0.01	100	−0.23	100	−0.04	100	−0.25	−0.06
4041.364	25.00	65					−0.05	hfs			−0.17	
4502.210	25.00		11	hfs	−0.14	100			0.06	hfs		+0.17
4761.507	25.00	19	19	hfs	−0.18	100			0.07	hfs		+0.19
4783.436	25.00	46	45	hfs	−0.18	100	−0.05	hfs	−0.01	hfs	−0.13	+0.11
4823.524	25.00	55	63	hfs	−0.25	100	−0.04	hfs	0.01	hfs	−0.13	+0.12
5377.637	25.00	11		hfs	+0.04	100	0.13	hfs			+0.05	
4604.982	28.00	24	33	−0.29	+0.05	100	−0.19	100	−0.13	100	−0.31	+0.03
4686.207	28.00	25		−0.64	+0.06	100	−0.07	100			−0.17	
4715.757	28.00		44	−0.34	+0.04	100			−0.01	100		+0.17
4752.415	28.00	19		−0.70	+0.03	100	−0.07	96			−0.18	
4754.756	28.00	9		−1.14	+0.17	100	−0.10	95			−0.24	
4904.407	28.00	45	49	−0.17	+0.12	100	−0.25	99	−0.09	100	−0.30	−0.01
4953.200	28.00	16		−0.67	+0.02	100	0.03	98			−0.05	
5017.568	28.00	30	33	−0.08	+0.09	100	−0.19	100	−0.20	100	−0.30	−0.08
5048.843	28.00	20	29	−0.38	+0.04	100	−0.16	99	0.06	98	−0.23	+0.15
5155.762	28.00		44	−0.09	+0.09	100			0.06	100		+0.15
5176.559	28.00	15	28	−0.44	+0.05	100	−0.10	99	0.09	100	−0.20	+0.17
5578.711	28.00	10	9	−2.64	+0.01	100			−0.05	91		+0.08
5593.733	28.00		18	−0.84	+0.07	100			0.17	100		+0.26
5663.975	28.00		11	−0.43	+0.07	100			0.21	97		+0.30
5754.655	28.00		27	−2.33	+0.27	100			0.11	100		+0.22
6086.276	28.00		16	−0.53	+0.10	100			0.13	100		+0.23
6108.107	28.00	10	19	−2.45	+0.03	100	0.05	100	0.13	100	−0.13	+0.31
6111.066	28.00	9		−0.87	+0.09	100	0.16	100			+0.06	
6176.807	28.00	19	29	−0.53	+0.33	100	−0.09	100	0.08	100	−0.18	+0.18
6378.247	28.00	9	10	−0.89	+0.09	100	0.20	100			+0.10	
6643.629	28.00	20	26	−2.30	+0.25	100	−0.04	99	−0.03	99	−0.21	+0.15
6767.768	28.00		29	−2.17	+0.28	100			−0.02	100		+0.16
6772.313	28.00	13	20	−0.98	+0.10	100	0.07	99	0.11	100	−0.05	+0.22
7522.758	28.00	20		−0.57	+0.15	100	−0.17	96			−0.30	
7525.111	28.00		29	−0.55	+0.05	100			−0.13	100		+0.00
7555.598	28.00	42	48	−0.05	+0.20	100	−0.28	100	−0.14	100	−0.40	−0.02
7574.043	28.00	20	33	−0.53	+0.10	100	−0.01	100	−0.02	100	−0.14	+0.11
7727.613	28.00		43	−0.17	+0.11	100			−0.16	100		−0.04
5218.197	29.00		25	hfs	−0.22	hfs			+0.11	hfs		+0.18
5220.066	29.00		10	hfs	−0.20	hfs			−0.01	hfs		+0.09
4722.153	30.00	30	37	−0.34	−0.14	100	+0.01	100	+0.22	100	−0.11	+0.33
4810.528	30.00			−0.14	−0.14	100	+0.21	100			+0.10	
4682.324	39.01			−1.51	+0.05	100	+0.46	100	+0.51	100	+0.32	+0.39

Table 5. continued.

λ (Å)	Code	Eq. width		log gf	Sun		Comp. A		Comp. B		A	B
		A	B		$\Delta\log gf$	%	$\Delta\log N$	%	$\Delta\log N$	%	mod B	mod A
1	2	3	4	5	6	7	8	9	10	11	12	13
5087.416	39.01	65	75	−0.17	−0.15	100	+0.35	100	+0.66	100	+0.19	+0.90
5509.895	39.01	20		−1.01	−0.13	97	+0.39	99			+0.27	
5662.925	39.01			0.16	+0.09	93	+0.23	98	+0.43	100	+0.14	+0.51
4208.977	40.01	50		−0.46	−0.05	100	+0.30	100			+0.14	
4379.742	40.01	35	30	−0.36	+0.11	99	+0.11	94	+0.23	98	+0.06	+0.25
4934.076	56.01	115		−0.16			+0.39	100			+0.26	
5853.668	56.01	50	65	−1.00	+0.17	100	+0.12	99	+0.25	100	−0.07	+0.44
6141.730	56.01	90	110	hfs			+0.18	hfs	+0.48	hfs	−0.02	+0.53
4562.359	58.01	15		+0.23	+0.01	99	+0.19	100			+0.10	

Column 1. Wavelengths (Å).
Column 2. Codes (neutral iron = 26.00).
Column 3. Equivalent widths of the lines in mÅ. Component A.
Column 4. Equivalent widths of the lines in mÅ. Component B.
Remark: equivalent widths were not used. Abundances were derived using spectrum synthesis method.
Column 5. Used oscillator strengths.
Column 6. Correction to the oscillator strengths from solar spectrum.
Column 7. Fraction of this line in the line absorbtion coefficient at the wavelength of the center of the line (percents) in the spectrum of the Sun.
Column 8. Differential abundance (relative to the corresponding line in the solar spectrum or to the mean solar abundance) of the element. Calculated for the line of the component A. The model with $T_{\rm eff}$ = 7450 K, log g = 4.0 was used.
Column 9. Fraction of this line in the line absorbtion coeffcient at the wavelength of the center of the line (percents) in the spectrum of the HD 153720 A.
Column 10. Differential abundance (relative to the corresponding line in the solar spectrum or to the mean solar abundance) of the element. Calculated for the line of the component B. The model with $T_{\rm eff}$ = 7125 K, log g = 3.9 was used.
Column 11. Fraction of this line in the line absorbtion coeffcient at the wavelength of the center of the line (percents) in the spectrum of the HD 153720 B.
Column 12. Differential abundance (relative to the corresponding line in the solar spectrum or to the mean solar abundance) of the element. Calculated for the line of the component A. The model with $T_{\rm eff}$ = 7125 K, log g = 3.9 was used.
Column 13. Differential abundance (relative to the corresponding line in the solar spectrum or to the mean solar abundance) of the element. Calculated for the line of the component B. The model with $T_{\rm eff}$ = 7450 K, log g = 4.0 was used.